Vibro-Acoustic Formulation of Elastically Restrained Shear Deformable Orthotropic Plates Using a Simple Shear Deformation Theory

A. Nayan and T.Y. Kam[*]

Mechanical Engineering Department, National Chiao Tung University, Hsin Chu 300, Taiwan

Abstract: A method is presented for vibro-acoustic analysis of elastically restrained orthotropic shear deformable plates subjected to excitation forces at different locations. The vibration of the shear deformable plate is formulated on the basis of the Ritz method and a simple first-order shear deformation theory in which 4 rather than 5 displacement components are used to simulate the deformation of the plate. The accuracy of the modal characteristics (natural frequency and mode shape) of an orthotropic plate predicted using the proposed method is verified by those obtained using other methods. The vibration responses of the plate are used in the first Rayleigh integral to construct the sound pressure level (SPL) curves of the plate subjected to excitation forces at different locations. The suitability of the present method for sound radiation analysis is validated by comparing the SPL curve obtained using the present method with those obtained using the other methods. The effects of different system parameters on the SPL curve of the plate are studied by means of several numerical examples. It has been shown that excitation location has significant effects on the smoothness of the SPL curve.

Keywords: Acoustics, orthotropic plate, vibration, Rayleigh-Ritz method, sound radiation.

1. INTRODUCTION

Recently, composite plates have found many applications in the engineering field. In particular, composite plates have been used in different industries such as aero-space, aircraft, automobile, and audio industries to fabricate structures or sound radiators of high performance and reliability. In general, these plates are flexibly restrained at their edges or connected at their edges to members which can be treated as elastic restraints. Since the vibration of a plate is susceptible to sound radiation, the vibro-acoustic behavior of plate structures has thus become an important topic of research. Recently, many papers [1-10] have been devoted to the vibro-acoustics of plates with regular boundary conditions subjected to various loads. Since, in practical applications, elastically restrained plates are important structural parts, a number of researchers have formulated some general methods for the vibro-acoustic analysis of elastically restrained rectangular thin isotropic plates [11-15]. Regarding the plate theories for the analysis of moderately thick plates, the traditional First-Order Shear Deformation Theory (FSDT), which considers 5 displacement components, introduced by Reissner [16] and Mindlin [17] has been widely used to study the deflection of plates. Kamand his associates have used this plate theory to study the vibro-acoustics of

composite plates [18,19]. Recently, a simple FSDT (termed SFSDT), which considers 4 displacement components, has been developed by Thai and Choi [20, 21] for bending and vibration analyses of laminated plates. The SFSDT, which can simplify the deflection analysis of moderate thick plates, may find applications insolving the iterative problems such as, for instance, optimal design, nonlinear analysis, and reliability analysis of plate structures. Therefore, it is worthy to explore the possible applications of the SFSDT in studying the vibro-acoustics of plates used for sound radiation.

In this paper, the vibro-acoustics, especially, the SPL curves of elastically restrained shear deformable orthotropic plates are studied using a method formulated on the basis of the SFSDT, the Ritz method, and the first Rayleigh integral. The modal characteristics (frequency and mode shape) as well as the SPL curves of a number of elastically restrained shear deformable orthotropic plates are determined using the proposed method. The effects of several system parameters on the SPL curves of the plates are also studied using the proposed method.

2. PLATE VIBRATION FORMULATION

The rectangular orthotropic plate of size *a* (length) × *b* (width) ×h_p (thickness) is elastically restrained along the plate periphery by distributed springs with translational and rotational spring constant intensities K_{Li} and K_{Ri}, respectively, and at the center by a spring of spring constant K_c as shown in Figure **1**. The x-y

*Address correspondence to this author at the Mechanical Engineering Department, National Chiao Tung University, Hsin Chu 300, Taiwan; Tel: +886-3-5712121; Fax: +886-3-6125057; E-mail: tykam@mail.nctu.edu.tw

plane of the reference coordinate is located at the mid-plane of the plate. Herein, the displacement of the plate is modeled based on the SFSDT. The displacement field of the plate is expressed as
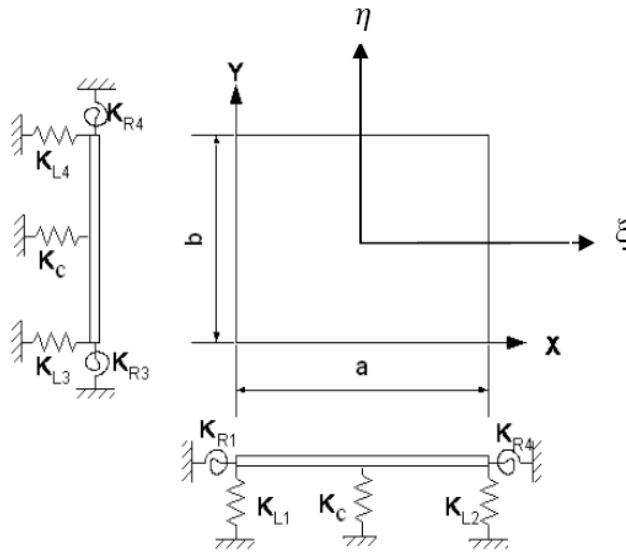

Figure 1: Orthotropic sound radiation plate.

$$u_p = u_{op}(x,y,t) - z_p \frac{\partial w_B}{\partial x}(x,y,t)$$

$$v_p = v_{op}(x,y,t) - z_p \frac{\partial w_B}{\partial y}(x,y,t) \qquad (1)$$

$$w_p = w_B(x,y,t) + w_S(x,y,t)$$

where u_p, v_p, and w_p are the displacements in x, y, and z directions, respectively; u_{op}, v_{op} are mid-plane displacements in x and y directions, respectively; w_B, w_S are mid-plane displacements in z direction due to bending and shear deformation, respectively. The strain-displacement relations of the plate are expressed as

$$\varepsilon_x = \frac{\partial u_{op}}{\partial x} - z_p \frac{\partial^2 w_B}{\partial x^2}$$

$$\varepsilon_y = \frac{\partial u_{op}}{\partial y} - z_p \frac{\partial^2 w_B}{\partial y^2}$$

$$\gamma_{xy} = \frac{\partial u_{op}}{\partial y} + \frac{\partial v_{op}}{\partial x} - 2z_p \frac{\partial^2 w_B}{\partial x \partial y} \qquad (2)$$

$$\gamma_{xz} = \frac{\partial w_S}{\partial x}$$

$$\gamma_{yz} = \frac{\partial w_S}{\partial y}$$

The stress-strain relations of the orthotropic plate are given as [22]

$$\begin{Bmatrix} \sigma_x \\ \sigma_y \\ \tau_{yz} \\ \tau_{xz} \\ \tau_{xy} \end{Bmatrix} = \begin{bmatrix} Q_{11} & Q_{12} & 0 & 0 & 0 \\ Q_{12} & Q_{22} & 0 & 0 & 0 \\ 0 & 0 & Q_{44} & 0 & 0 \\ 0 & 0 & 0 & Q_{55} & 0 \\ 0 & 0 & 0 & 0 & Q_{66} \end{bmatrix} \begin{Bmatrix} \varepsilon_x \\ \varepsilon_y \\ \gamma_{yz} \\ \gamma_{xz} \\ \gamma_{xy} \end{Bmatrix} \qquad (3)$$

with

$$Q_{11} = \frac{E_1}{1 - v_{12}v_{21}}$$

$$Q_{12} = \frac{v_{12}E_2}{1 - v_{12}v_{21}}$$

$$Q_{22} = \frac{E_2}{1 - v_{12}v_{21}} \qquad (4)$$

$$Q_{44} = G_{23}$$

$$Q_{55} = G_{13} = G_{12}$$

$$Q_{66} = G_{12}$$

where Q_{ij} is reduced stiffness constant, E_i is Young's modulus in the ith direction, v_{ij} is Poisson's ratio, and G_{ij} is shear modulus.

The strain energy, U_p, of the plate is

$$U_P = \frac{1}{2} \int_{V_p} \left(\sigma_x \varepsilon_x + \sigma_y \varepsilon_y + \tau_{xy} \gamma_{xy} + \tau_{xz} \gamma_{xz} + \tau_{zy} \gamma_{yz} \right) dV_p \qquad (5)$$

In view of the relations given in eqns (1)-(4), eqn (5) can be rewritten as

$$U_p = \frac{1}{2} \int_0^a \int_0^b \begin{bmatrix} Q_{11} h_p \left(\frac{\partial u}{\partial x}\right)^2 + Q_{11} \frac{h_p^3}{12} \left(\frac{\partial^2 w_B}{\partial x^2}\right)^2 + 2Q_{12} h_p \left(\frac{\partial u}{\partial x}\right)\left(\frac{\partial v}{\partial y}\right) \\ +2Q_{12} \frac{h_p^3}{12} \left(\frac{\partial^2 w_B}{\partial x^2}\right)\left(\frac{\partial^2 w_B}{\partial y^2}\right) + Q_{22} h_p \left(\frac{\partial v}{\partial y}\right)^2 + Q_{22} \frac{h_p^3}{12} \left(\frac{\partial^2 w_B}{\partial y^2}\right)^2 \\ +2Q_{66} h_p K_p \left(\frac{\partial u}{\partial y}\right)\left(\frac{\partial v}{\partial x}\right) + Q_{66} h_p K_p \left(\frac{\partial u}{\partial y}\right)^2 + Q_{66} h_p K_p \left(\frac{\partial v}{\partial x}\right)^2 + \\ Q_{66} K_p \frac{h_p^3}{3} \left(\frac{\partial^2 w_B}{\partial x \partial y}\right)^2 + Q_{55} h_p K_p \left(\frac{\partial w_S}{\partial x}\right)^2 + Q_{44} h_p K_p \left(\frac{\partial w_S}{\partial y}\right)^2 \end{bmatrix} dy dx \qquad (6)$$

where K_p is shear correction factor which is generally assumed to be 0.85.

The kinetic energy, T_p, of the plate is

$$T_P = \frac{1}{2} \int_{V_p} \rho_p \left(\dot{u}_p^2 + \dot{v}_p^2 + \dot{w}_p^2 \right) dV_p \qquad (7)$$

where ρ_p is plate mass density. In view of eqn (1), the above equation can be rewritten as

$$T_p = \frac{1}{2}\int_0^b \int_0^a \rho_p \begin{bmatrix} h_p\left(\dfrac{\partial u_{op}}{\partial t}\right)^2 + h_p\left(\dfrac{\partial v_{op}}{\partial t}\right)^2 + h_p\left(\dfrac{\partial w_B}{\partial t}\right)^2 + \\ h_p\left(\dfrac{\partial w_S}{\partial t}\right)^2 + 2h_p\left(\dfrac{\partial w_B}{\partial t}\right)\left(\dfrac{\partial w_S}{\partial t}\right) + \\ \dfrac{h_p^3}{12}\left(\dfrac{\partial^2 w_B}{\partial t \partial x}\right)^2 + \dfrac{h_p^3}{12}\left(\dfrac{\partial^2 w_B}{\partial t \partial x}\right)^2 \end{bmatrix} dxdy \quad (8)$$

The strain energy, U_S, stored in the elastic restraints is written as

$$U_S = \frac{K_{L1}}{2}\int_0^b w^2\Big|_{x=0} dy + \frac{K_{L2}}{2}\int_0^b w^2\Big|_{x=0} dy + \frac{K_{L3}}{2}\int_0^b w^2\Big|_{x=0} dy$$
$$+ \frac{K_{L4}}{2}\int_0^b w^2\Big|_{x=0} dy + \frac{K_{R1}}{2}\int_0^b \frac{\partial w}{\partial x}\Big|_{x=0} dy + \frac{K_{R2}}{2}\int_0^b \frac{\partial w}{\partial x}\Big|_{x=0} dy \quad (9)$$
$$+ \frac{K_{R3}}{2}\int_0^b \frac{\partial w}{\partial y}\Big|_{x=0} dy + \frac{K_{R4}}{2}\int_0^b \frac{\partial w}{\partial y}\Big|_{x=0} dy + K_C w\left(\frac{a}{2},\frac{b}{2}\right)^2$$

The total strain energy U of the elastically restrained plate is the sum of U_p and U_s.

The Rayleigh-Ritz method is used to study the free vibration of the elastically restrained stiffened plate. The displacements of the plate are expressed as

$$\begin{aligned} u_{op}(x,y,t) &= U(x,y)\sin\omega t \\ v_{op}(x,y,t) &= V(x,y)\sin\omega t \\ w_B(x,y,t) &= W_b(x,y)\sin\omega t \\ w_S(x,y,t) &= W_S(x,y)\sin\omega t \end{aligned} \quad (10)$$

with

$$U(\xi,\eta) = \sum_{i=1}^{\hat{A}}\sum_{j=1}^{\hat{B}} C_{ij}\phi_i(\xi)\psi_j(\eta)$$
$$V(\xi,\eta) = \sum_{i=1+\hat{A}}^{\hat{C}}\sum_{j=1+\hat{B}}^{\hat{D}} C_{ij}\phi_i(\xi)\psi_j(\eta)$$
$$W_B(\xi,\eta) = \sum_{i=1+\hat{C}}^{\hat{I}}\sum_{j=1+\hat{D}}^{\hat{J}} C_{ij}\phi_i(\xi)\psi_j(\eta) \quad (11)$$
$$W_S(\xi,\eta) = \sum_{i=1+\hat{I}}^{\hat{M}}\sum_{j=1+\hat{J}}^{\hat{N}} C_{ij}\phi_i(\xi)\psi_j(\eta)$$

where C_{ij} are unknown constants; $\hat{A},\hat{B},\hat{C},\hat{D},\hat{I},\hat{J},\hat{M},\hat{N}$ denote the numbers of terms in the series. Legendre's polynomials are used to represent the characteristic functions, ϕ and ψ. Let $\xi=2x/a$-1 and $\eta=2y/b$-1. The normalized characteristic functions, for instance, $\phi_i(\xi)$, are given as

$$\begin{aligned} \phi_1(\xi) &= 1, \\ \phi_2(\xi) &= \xi, \end{aligned} \quad -1 \le \xi \le 1 \quad (12)$$

for n≥3,

$$\phi_n(\xi) = [(2n-3)\xi \times \phi_{n-1}(\xi) - (n-2) \times \phi_{n-2}(\xi)]/(n-1)$$

with the satisfaction of the following orthogonality condition:

$$\int_{-1}^1 \phi_n(\xi)\phi_m(\xi)d\xi = \begin{cases} 0 & ,\text{if} \quad n \ne m \\ \dfrac{2}{2n-1} & ,\text{if} \quad n = m \end{cases} \quad (13)$$

Extremization of the functional $\Pi=T-U$ gives the following eigenvalue problem.

$$[K - \omega^2 M]C = 0 \quad (14)$$

where **K** and **M** are structural stiffness and mass matrices; ω is circular frequency. The solution of the above eigenvalue problem can lead to the determination of the natural frequencies and mode shapes of the plate. The terms in **K** and **M** are listed in the appendix.

3. PLATE SOUND RADIATION ANALYSIS

The modal characteristics obtained in the previous section can be used to study the force vibration and sound radiation of the elastically restrained plate. For a sound radiation panel excited by an electro-magnetic transducer with a cylindrical voice coil of radius r_c, the harmonic driving force $F(t) = F_o \sin\omega t$ acting on the bottom surface of the plate is distributed uniformly around a circle of radius r_c.

The equations of motion for the sound radiation plate subjected to forced vibration can be expressed as

$$\underline{M\ddot{C}} + \underline{D\dot{C}} + \underline{KC} = \underline{F} \quad (15)$$

where **F** is the force vector containing the following terms

$$F_{mn} = \frac{F_o}{2\pi r_c}\int_0^{2\pi} \phi_m\left(\frac{2r_c}{a}\cos\theta\right)\varphi_n\left(\frac{2r_c}{b}\cos\theta\right)d\theta \sin\omega t, \quad (16)$$
$$for \quad m = 1+\hat{I},...,\hat{M}; n = 1+\hat{J},...,\hat{N} = 0 \, for \, other \, m,n$$

It is noted that the contributions of w_B and w_S to the work done by the applied force have been considered in deriving the above equation. The damping matrix D is

$$[D] = \alpha[M] + \beta[K] \quad (17)$$

with $\alpha = \zeta \omega$, $\beta = 2\zeta/\omega$ where ζ is damping ratio at the first resonant frequency of the elastically restrained plate. Equation (17) can be solved using the modal analysis method. Consider the case in which the plate is excited by line loads oriented in the x-direction. For a line load of length L_f and constant intensity located at the central area of the plate with y = b/2, the terms in **F** are expressed as

$$F_{mn} = \frac{aF_o}{2L_f} \int_{-\frac{L_f}{a}}^{\frac{L_f}{a}} \phi_m(\xi)\varphi_n(0) d\xi \sin \omega t \tag{18a}$$

and for two line loads in parallel toward the x direction,

$$F_{mn} = \frac{aF_o}{2L_f} \left\{ \phi_m(-\eta_1)\int_{-\frac{L_f}{a}}^{\frac{L_f}{a}} \varphi_n(\xi) d\xi + \phi_m(\eta_2)\int_{-\frac{L_f}{a}}^{\frac{L_f}{a}} \varphi_n(\xi) d\xi \right\} \tag{18b}$$

$$\text{for } m = 1+\hat{I},...,\hat{M}; n = 1+\hat{J},...,\hat{N} = 0 \text{ for other } m,n$$

Referring to the baffled plate with area *S* shown in Figure **2**, if the effects of air loading on the plate vibration are neglected, the sound pressure p(r, t) resulting from the vibration of the plate can be determined using the first Rayleigh integral.

$$p(r,t) = \frac{-\varpi^2 \rho_0}{2\pi} \sum_i A_i e^{j(2\varpi t+\theta i - kRi)} \frac{\Delta Si}{R_i} \tag{19}$$
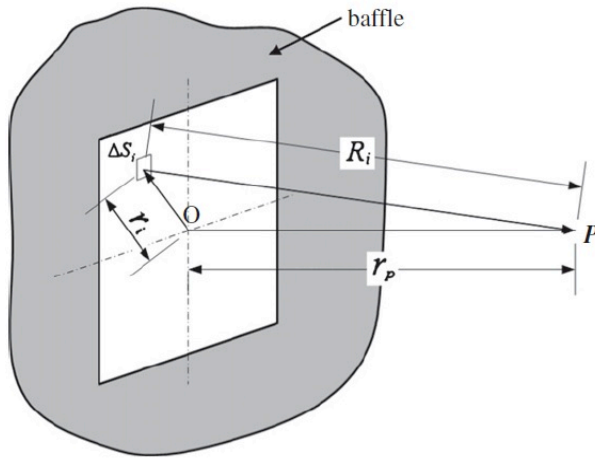
Figure 2: Sound pressure measurement of baffled plate.

where ρ_0 is air density; *k* is wave number ($= \varpi / c$) with *c* being speed of sound; *r* is the distance between the plate center and the point of measurement; $R_i = |r_p - r_i|$ the distance between the observation point and the position of the surface element at r_s; θ is phase angle; $j = \sqrt{-1}$. For air at 20°C and standard

atmospheric pressure, $\rho_0 = 1.2 \, kg/m^3$ and $c = 344 \, m/s$. The SPL produced by the plate is calculated as

$$SPL \equiv 20\log_{10}\left(\frac{p_{rms}}{2\times10^{-5}}\right) dB \tag{20}$$

with

$$p_{rms} = \left[\frac{1}{T}\int_{-T/2}^{T/2}|p(r,t)|^2 \, dt\right]^{1/2} \tag{21}$$

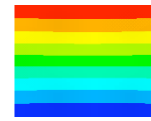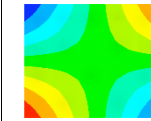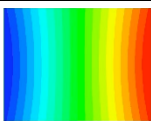It is noted that both eqns (19) and (21) are solved numerically.
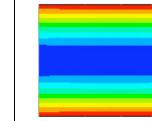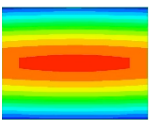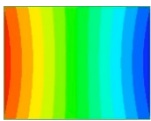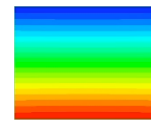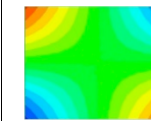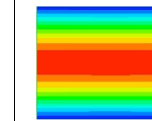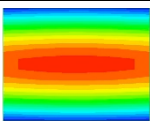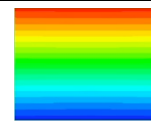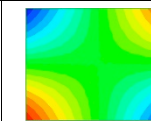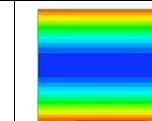
Table 1:   Properties of Orthotropic Plate

Material constants	Plate	Surround
E_1 (GPa)	3.7	
E_2 (GPa)	0.055	
v_{12}	0.03	
v_{23}	0.2	
v_{13}	0.03	
G_{12} (GPa)	0.05	
G_{23} (GPa)	0.05/6	
G_{13} (GPa)	0.05	
ρ(kg/m³)	300	
K_C (N/m²)		1654.4
K_L (N/m²)		4744.7
K_R (N)		0

4. RESULTS AND DISCUSSIONS

The proposed vibration formulation is first applied to analyze the free vibration of an elastically restrained orthotropic plate of size 26.5 mm × 20.5 mm × 1 mm. The properties of the plate, spring constant intensity of the surround, and spring constant of the central support are listed in Table **1**. For comparison purpose, the plate is also analyzed using two other methods, namely, the finite element code ANSYS [23] and the method formulated based on the conventional FSDT [24]. In the ANSYS finite element analysis, Shell99 elements and Combin14 elements are used to simulate the plate and springs, respectively. In the Rayleigh-Ritz methods based on the conventional FSDT and SFSDT, 10 terms for each displacement characteristic function are used in the free vibration analysis. The modal characteristics (frequency and mode shape) of the first 5 modes determined using different methods are tabulated in Table **2** for comparison. It is noted that all the results are in good agreement. In particular, the largest

Table 2:   Mode Shape and Natural Frequency of Orthotropic Sound Radiating Plate

Method		Mode no.				
		1	**2**	**3**	**4**	**5**
ANSYS	Mode shape					
	Natural Freq.(Hz)	354.80	511.5	541.12	1073.4	1339.2
FSDT [24]	Mode shape					
	Natural Freq.(Hz)	354.6	509.9	541.2	1071	1333
	Difference (%)*	0.06%	0.31%	0.01%	0.22%	0.47%
SFSDT	Mode shape					
	Natural Freq.(Hz)	354.9	510.8	542.4	1100	1351
	Difference (%)*	0.03%	0.14%	0.24%	2.48%	0.88%

*Difference (%) = 100x (ANSYS value - other value)/ANSYS value %.

percentage discrepancy between the fourth natural frequency determined from the finite element method and that from the SFSDT is only 2.88%. The sound radiation of the orthotropic plate is also studied using the present method. The SPL curves constructed using the vibration responses determined from different methods are shown in Figure **3** for comparison. It is noted that the fact of the SPL curves being almost the same, especially in the frequency range from 20 Hz to 4 kHz, has demonstrated the suitability of the present method for sound radiation analysis of panel-form sound radiators. It is also worthy to note that the SPL dip at around 1.5 kHz is induced by the first vibration mode shape of the plate.

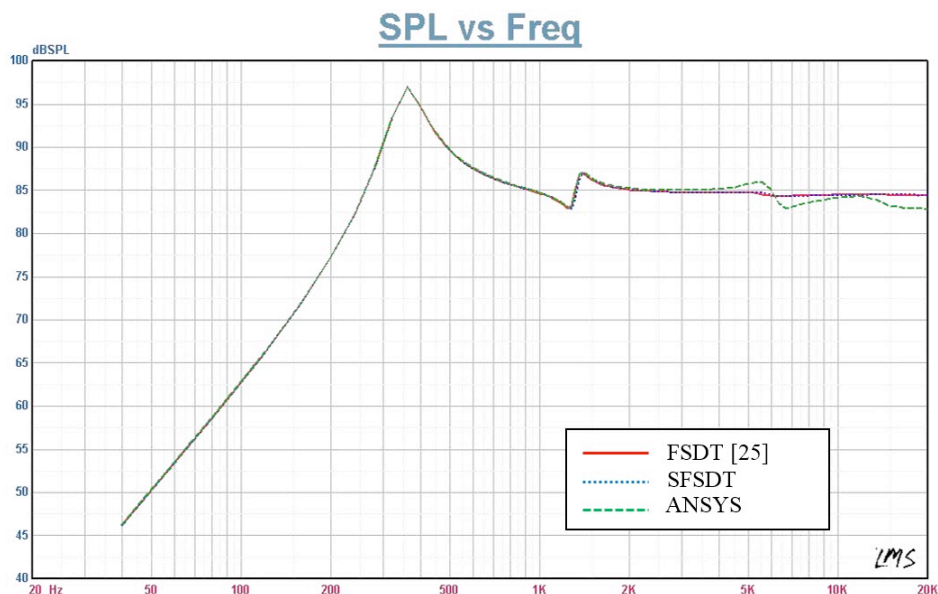Next, study how the system parameters such as plate thickness, elastic modulus ratio, and excitation

Figure 3: SPL curves of orthotropic plate (h = 1 mm) determined using different methods.
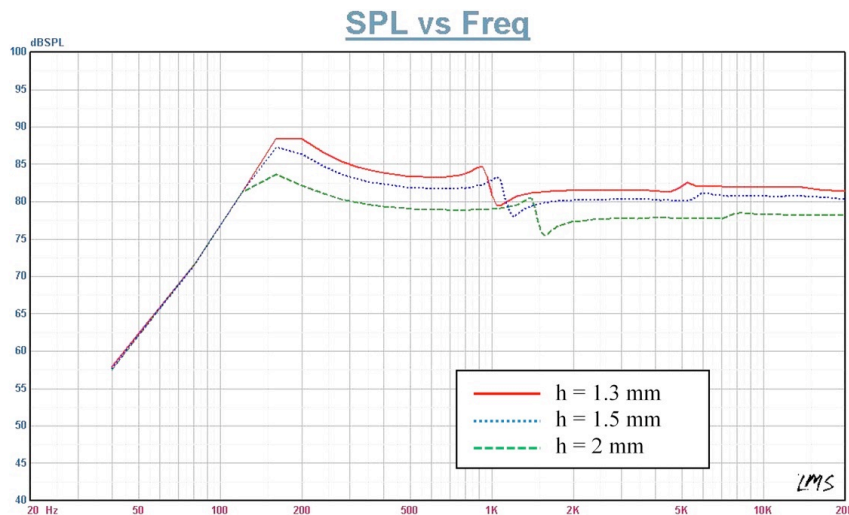
Figure 4: SPL curves of orthotropic plate with different thicknesses (a/b = 2.92).

location affect the SPL curve, especially the first SPL dip of an orthotropic flat-panel sound radiator. Consider the above orthotropic plate of aspect ratio *a/b* = 2.92 with *a* = 76 *mm*, *b* = 26 *mm*. The SPL curves of the plate with different thicknesses (h_p), ie, 1.3 mm, 1.5 mm, and 2 mm are determined using the present method as shown in Figure **4**. It is noted that the plate thickness has a direct effect on the magnitude of the SPL curve, i.e, the thicker the plate, the lower the SPL. It is also noted that the first SPL dip frequencies for the plate thicknesses of 1.3, 1.5, and 2 mm are 900, 1100, and 1500 Hz, respectively. Therefore, the increase in plate thickness can increase the plate stiffness which in turn makes the first SPL dip frequency higher. The effects of the elastic modulus ratio, E_1/E_2 on the plate SPL curve are to be studied. Setting E_2 = 0.055GPa, the SPL curves for E_1/E_2 = 1, 2, and 3 are shown in Figure **5** for comparison. The small variations of the SPL curves in the audible frequency range for these cases have demonstrated the fact that E_1/E_2 has negligible effects on the SPL curve behavior. Finally, the effects of excitation location on the SPL curve of the plate are studied using the present method. The SPL curves of the plate excited by, respectively, a circular force of radius r_c = 9.35 mm at the plate center, one-line load, and two-line load are shown in Figure **6**. The total force F_o for the three cases is 0.58415 N. For the one-line load case, the load with length L_f = 18.7 mm is acting at the central area of the plate. The two line loads with length L_f = 18.7 mm are oriented in the x-direction and located at the central area of the plate with y- coordinates y_1 = -9.35mm and y_2 = 9.35 mm, respectively. As shown in Figure **6**, the first SPL dip frequencies of the three cases are around 1.35kHz but

the SPL dip magnitude of the one-line load case is much larger than those of the circular load and two-line load cases. The vibration mode shape for the first SPL dip frequency is shown in Table **2**. Beyond the first SPL dip frequency, the SPL curve of the circular load case is very smooth while both the SPL curves of the one-line and two-line load cases have an other SPL dips at around 5889 Hz. The vibration shapes of the plate at the second SPL dip frequency for different load cases are shown in Figure **7** for comparison. It is noted that in view of the vibration shapes of the load cases, the shape of the circular load case has the smallest opposite phase area which can thus lead to the smoothness of the SPL curve in that frequency range. Therefore, for this orthotropic flat-panel sound radiator, the location of the circular load case can produce the best SPL curve. In view of the above SPL curves of the plate obtained using different system parameters, it is clear that the excitation location may have significant beneficial effects on the SPL curve of the plate. Therefore, it is worthy to study the optimal excitation locations for different composite flat-panel sound radiators in the future.

5. CONCLUSION

A method based on the Rayleigh-Ritz method and the Rayleigh first integral has been developed for the vibro-acoustic analysis of elastically restrained shear deformable orthotropic rectangular plates. The simple FSDT composed of 4 displacement components has been used to formulate the vibration of the shear deformable plate. The accuracy of the proposed method in predicting the modal characteristics and SPL curve of an elastically restrained orthotropic plate of
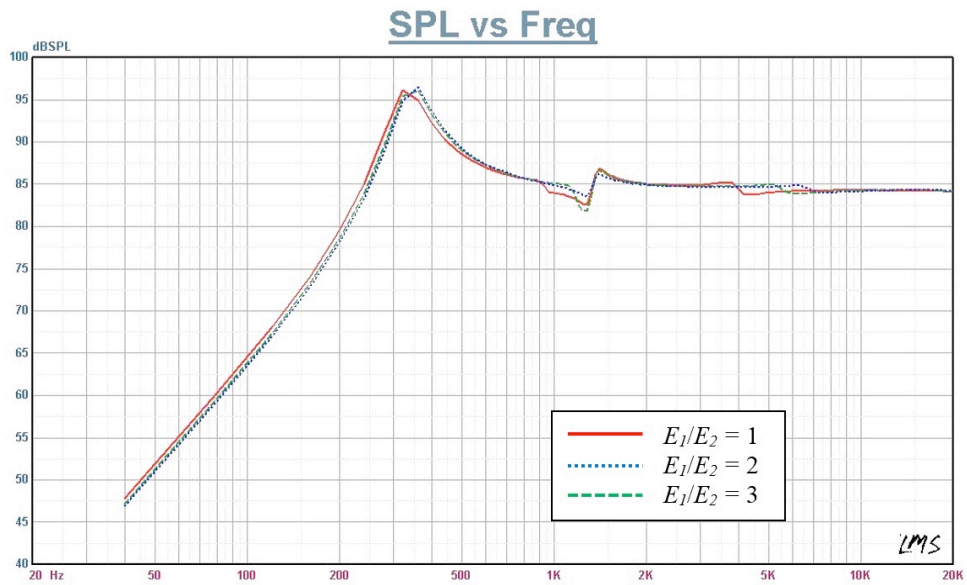
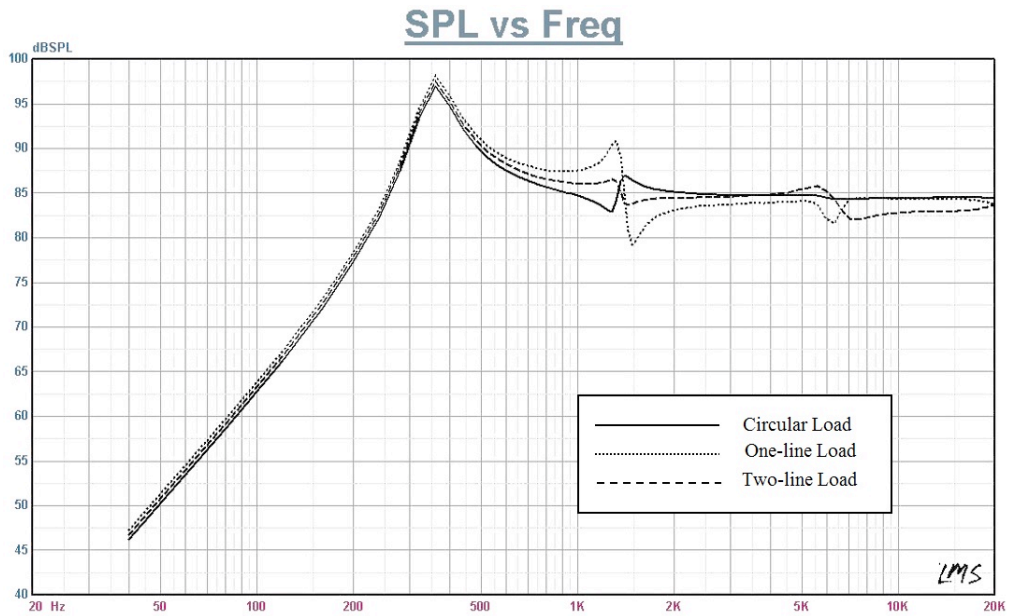**Figure 5:** SPL curves of orthotropic plate with different E_1/E_2 ratios (a/b = 1.25, E2 = 0.055 GPa).

Figure 6: SPL curves produced by excitation force at different locations.

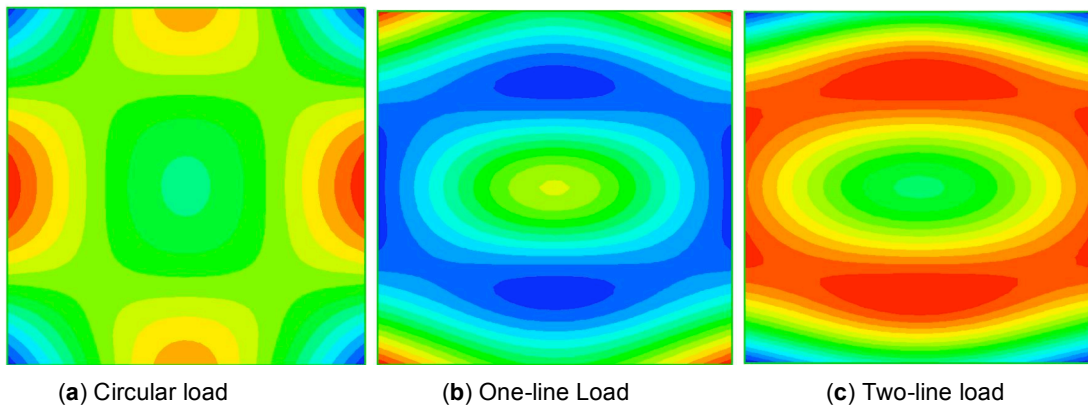(**a**) Circular load   (**b**) One-line Load   (**c**) Two-line load

Figure 7: Vibration shape at the second SPL dip frequency (5889 Hz).

aspect ratio *a/b* = 1.3 has been verified by those obtained using other methods. The effects of thickness, Young's modulus ratio E_1/E_2, and excitation location on the SPL curve of an elastically restrained rectangular orthotropic plate of aspect ratio *a/b* = 2.92 have been studied using the proposed method. It has been found that the increase in plate thickness can decrease the SPL and slightly increase the first SPL dip frequency, the effects of Young's modulus ratio on the SPL curve of the plate is negligible, and the location of excitation force may have significant beneficial effects on the SPL curve of the plate.

ACKNOWLEDEGEMENT

APPENDIX A

$$\left(\begin{bmatrix} K_{11} & 0 & 0 & 0 \\ 0 & K_{22} & 0 & 0 \\ 0 & 0 & K_{33} & K_{34} \\ 0 & 0 & K_{43} & K_{44} \end{bmatrix} - \omega^2 \begin{bmatrix} M_{11} & 0 & 0 & 0 \\ 0 & M_{22} & 0 & 0 \\ 0 & 0 & M_{33} & 0 \\ 0 & 0 & 0 & M_{44} \end{bmatrix} \right) \quad \text{(A1)}$$

$$\begin{Bmatrix} C_{ij} \\ C_{mn} \\ C_{ab} \\ C_{cd} \end{Bmatrix} = \begin{Bmatrix} 0 \\ 0 \\ 0 \\ 0 \end{Bmatrix}$$

$$\left[K^{11} \right]_{ij\bar{i}\bar{j}} = \frac{1}{2} \begin{bmatrix} Q_{11} \dfrac{h_p^{\,3}}{3} \dfrac{2b}{a^3} E^{22} F^{00} + 2Q_{12} \dfrac{h_p^{\,3}}{3} \dfrac{1}{ab}\left(E^{20}F^{02} + E^{02}F^{20}\right) \\[2mm] + Q_{22} \dfrac{h_p^{\,3}}{3} \dfrac{2a}{b^3} E^{00}F^{22} + Q_{66}k_p \dfrac{h_p^{\,3}}{3}\dfrac{8}{ab}E^{11}F^{11} \end{bmatrix}$$

$$+ \frac{1}{2}\begin{bmatrix} K_{L1}bF^{00}BB^{00} + K_{L2}bF^{00}BB^{00} + \\[1mm] K_{L3}aE^{00}BB^{00} + K_{L4}aE^{00}BB^{00} + K_C E^{00}F^{00} \end{bmatrix} \quad \text{(A2)}$$

$$\left[K^{22} \right]_{mn\bar{m}\bar{n}} = \frac{1}{2}\left[Q_{55}K_p h_p \frac{2b}{a} E^{11}F^{00} + Q_{44}K_p h_p \frac{2a}{b} E^{00}F^{11} \right]$$

$$\left[K^{33} \right]_{ab\bar{a}\bar{b}} = \frac{1}{2}\left[Q_{11}h_p \frac{2b}{a} E^{11}F^{00} + Q_{66}K_p h_p \frac{2a}{b} E^{00}F^{11} \right]$$

$$\left[K^{33} \right]_{abcd} = \frac{1}{2}\left[2Q_{12}h_p E^{01}F^{10} + 2Q_{66}K_p h_p E^{10}F^{01} \right]$$

$$\left[K^{44} \right]_{cd\bar{c}\bar{d}} = \frac{1}{2}\left[Q_{22}h_p \frac{2a}{b} E^{00}F^{11} + Q_{66}K_p h_p \frac{2b}{a} E^{11}F^{00} \right]$$

and

$$\left[M^{11} \right]_{ij\bar{i}\bar{j}} = \rho_p h_p^{\,3} \frac{b}{12a} E^{10}F^{00} + \rho_p h_p^{\,3} \frac{a}{12b}$$

$$E^{00}F^{10} + \rho_p h_p^{\,3} \frac{ab}{4} E^{00}F^{00}$$

$$\left[M^{22} \right]_{mn\bar{m}\bar{n}} = \rho_p h_p \frac{ab}{4} E^{00}F^{00} \quad \text{(A3)}$$

$$\left[M^{33} \right]_{ab\bar{a}\bar{b}} = \rho_p h_p \frac{b}{4} E^{00}F^{00}$$

$$\left[M^{44} \right]_{cd\bar{c}\bar{d}} = \rho_p h_p \frac{ab}{4} E^{00}F^{00}$$

where

$$r, s = 0, 1;$$
$$i, j, \bar{i}, \bar{j} = 1, 2, 3, \dots I, J$$
$$m, n, \bar{m}, \bar{n} = 1, 2, 3, \dots M, N$$
$$a, b, \bar{a}, \bar{b} = 1, 2, 3, \dots C, D$$

$$E^{rs}_{im} = \int_{-1}^{1}\left[\frac{d^r\phi(\xi)}{d\xi^r}\frac{d^s\phi(\xi)}{d\xi^s}\right]d\xi$$

$$F^{rs}_{jn} = \int_{-1}^{1}\left[\frac{d^r\psi(\eta)}{d\eta^r}\frac{d^s\psi(\eta)}{d\eta^s}\right]d\eta \quad \text{(A4)}$$

REFERENCES

[1]   Li S. Active modal control simulation of vibro-acoustic response of a fluid-loaded plate. J Sound Vib 2011; 330(23): 5545-57.
http://dx.doi.org/10.1016/j.jsv.2011.07.001

[2]   Putra A, Thompson DJ. Radiation efficiency of unbaffled and perforated plates near a rigid reflecting surface. J Sound Vib. 2011; 330(22): 5443-59.
http://dx.doi.org/10.1016/j.jsv.2011.05.033

[3]   Jeyaraj P, Padmanabhan C, Ganesan N. Vibro-acoustic behavior of a multilayered viscoelastic sandwich plate under a thermal environment. J Sandw Struct Mater 2011 Jul; 13(5): 509-37.
http://dx.doi.org/10.1177/1099636211400129

[4]   Inalpolat M, Caliskan M, Singh R. Analysis of near field sound radiation from a resonant unbaffled plate using simplified analytical models. Noise Control Eng Ldots [Internet] 2010; Available from. http://www.ingentaconnect.com/content/ince/ncej/2010/00000058/00000002/art00004

[5]   Franco F, De Rosa S, Polito T. Finite Element Investigations on the Vibroacoustic Performance of Plane Plates with Random Stiffness. Mech Adv Mater Struct 2011; 18(7): 484-97.
http://dx.doi.org/10.1080/15376494.2011.604602

[6]   Sorokin SV. Vibrations of and sound radiation from sandwich plates in heavy fluid loading conditions. Compos Struct 2000; 48(4): 219-30.
http://dx.doi.org/10.1016/S0263-8223(99)00103-8

[7]   Zhang X, Li WL. A unified approach for predicting sound radiation from baffled rectangular plates with arbitrary boundary conditions. J Sound Vib 2010; 329(25): 5307-20.
http://dx.doi.org/10.1016/j.jsv.2010.07.014

[8]   Bert CW, Kim CD, Birman V. Vibration of composite-material cylindrical shells with ring and/or stringer stiffeners. Compos

Struct 1993; 25: 477-84.
http://dx.doi.org/10.1016/0263-8223(93)90195-V

[9]   Mittelstedt C, Beerhorst M. Closed-form buckling analysis of compressively loaded composite plates braced by omega-stringers. Compos Struct 2009; 88(3): 424-35.
http://dx.doi.org/10.1016/j.compstruct.2008.05.021

[10]   Zhang Z, Chen H, Ye L. Progressive failure analysis for advanced grid stiffened composite plates/shells. Compos Struct 2008; 86(1-3): 45-54.
http://dx.doi.org/10.1016/j.compstruct.2008.03.037

[11]   Xin FX, Lu TJ. Analytical modeling of wave propagation in orthogonally rib-stiffened sandwich structures: Sound radiation. Comput Struct 2011 Mar; 89(5-6): 507-16.

[12]   Cao X, Hua H, Zhang Z. Sound radiation from shear deformable stiffened laminated plates. J Sound Vib 2011; 330: 4047-63.
http://dx.doi.org/10.1016/j.jsv.2011.04.016

[13]   Legault J, Mejdi A, Atalla N. Vibro-acoustic response of orthogonally stiffened panels: The effects of finite dimensions. J Sound Vib 2011; 330(24): 5928-48.
http://dx.doi.org/10.1016/j.jsv.2011.07.017

[14]   Xu H, Du J, Li WL. Vibrations of rectangular plates reinforced by any number of beams of arbitrary lengths and placement angles. J Sound Vib 2010; 329(18): 3759-79.
http://dx.doi.org/10.1016/j.jsv.2010.03.023

[15]   Xin FX, Lu TJ. Sound radiation of orthogonally rib-stiffened sandwich structures with cavity absorption. Compos Sci Technol 2010; 70(15): 2198-206.
http://dx.doi.org/10.1016/j.compscitech.2010.09.001

[16]   Reissner E. The effect of transverse shear deformation on the bending of elastic plates. J Appl Mech 1945; 12(2): 69-77.

[17]   Mindlin RD. Influence of Rotatory Inertia and Shear on Flexural Motions of Isotropic, Elastic Plates. J Appl Mech-Trans ASME 1951; 18: 31-8.

[18]   Kam TY, Jiang CH, Lee BY. Vibro-acoustic formulation of elastically restrained shear deformable stiffened rectangular plate. Compos Struct 2012; 94(11): 3132-41.
http://dx.doi.org/10.1016/j.compstruct.2012.04.031

[19]   Jiang CH, Chang YH, Kam TY. Optimal design of rectangular composite flat-panel sound radiators considering excitation location. Compos Struct 2014; 108(1): 65-76.

[20]   Thai HT, Choi DH. A simple first-order shear deformation theory for laminated composite plates. Compos Struct 2013; 106: 754-63.
http://dx.doi.org/10.1016/j.compstruct.2013.06.013

[21]   Thai HT, Choi DH. A simple first-order shear deformation theory for the bending and free vibration analysis of functionally graded plates. Compos Struct 2013; 101: 332-40.
http://dx.doi.org/10.1016/j.compstruct.2013.02.019

[22]   Jones RM. Mechanics of composite material. McGraw-Hill Inc.: New York 1975.

[23]   ANSYS 12.1. ANSYS Inc. USA 2010.

[24]   Li BY. Vibration and Sound Radiation of Laminated Composite Plates Considering the Effects of Shear Deformation and Attached Masses [Thesis]. [Taiwan]. National Chiao Tung Univeristy 2011.